Compressive sampling for multispectral imaging in the vis-NIR-TIR: optical design of space telescopes

G. Pariani, A. Zanutta, M. Genoni, S. Basso, A. Bianco, et al.

G. Pariani, A. Zanutta, M. Genoni, S. Basso, A. Bianco, M. Benetti, R. Freddi, V. Striano, G. Cilia, S. Sanguinetti, R. Colombo, "Compressive sampling for multispectral imaging in the vis-NIR-TIR: optical design of space telescopes," Proc. SPIE 10698, Space Telescopes and Instrumentation 2018: Optical, Infrared, and Millimeter Wave, 106985O (6 July 2018); doi: 10.1117/12.2312008

SPIE.

Event: SPIE Astronomical Telescopes + Instrumentation, 2018, Austin, Texas, United States

Compressive sampling for multispectral imaging in the vis-NIR-TIR: optical design of space telescopes

G. Pariani[a*], A. Zanutta[a], M. Genoni[a], S. Basso[a], A. Bianco[a], M. Benetti[b], R. Freddi[b], V. Striano[b], G. Cilia[c], S. Sanguinetti[d], R. Colombo[e]

[a] INAF, Osservatorio Astronomico di Brera, via E. Bianchi 46, 23807 Merate (Italy); [b] OHB Italia S.p.A., Via Gallarate 150, 20151 Milano (Italy); Antares S.c.a.r.l., Via Gallarate 150, 20151 Milano (Italy); [c] OPTEC S.p.A., Via Mantegna 34, 20015 Parabiago (Italy); [d] L-NESS and Dipartimento di Scienza dei Materiali, Universita' degli Studi di Milano-Bicocca, Via R. Cozzi 55, 20125 Milano (Italy); [e] Remote Sensing of Environmental Dynamics Lab., DISAT, Università di Milano-Bicocca, P.zza della Scienza 1, 20126 Milano (Italy).

ABSTRACT

Micro-satellites equipped with multispectral payloads are now under development to acquire information on the radiation reflected and emitted from the earth in the vis-NIR-TIR bands. In this framework, we are studying different approaches based on the compressive sampling technique supported by innovative multispectral detectors, where the image sampling is performed on the telescope focal plane with a Digital Micromirror Device (DMD). We will describe in the paper the possibilities and the constraints given by the use of the DMD in the focal plane. The optical design of the telescope, relay system and detector in two different application cases will be provided.

Keywords: compressive sampling, multispectral imaging, vis-NIR-TIR, DMD, micro-satellites, space telescope.

1. INTRODUCTION

Multispectral imaging is of great importance in earth observations for environmental and cryosphere monitoring applications. Most of the cryosphere components exists very near their limit of phase transition from solid to liquid. For this reason, the study of their melting dynamics represents a fundamental task of current scientific research, in particular in the context of current increase of atmospheric temperature. At the moment, different NASA and ESA satellite missions are devoted to the study of the cryosphere (e.g. Landsat[1], Terra/Aqua[2], Cryosat[3], Sentinel[4], etc.), but no sensor features a high spatial and spectral resolution in the thermal and optical domains. Micro-satellites are now under development to acquire information on the radiation reflected and emitted from the earth in the vis-NIR (0.4-1.7um) and TIR bands (up to 12 um).

In this framework, we are studying different approaches based on the compressive sampling technique for collecting high quality multispectral images. Compressive sampling is an imaging technique based on the measurement of the integrated flux obtained from a random sample of the image, which recovers the image from far fewer measurements than traditional methods do. This technique relies on two principles: sparsity, which pertains to the signals of interest, and incoherence, which pertains to the sensing modality[5]. To exploit this technique for compressing data while acquiring, the collected light must be modulated through multiple random patterns, each one collected as a single reading. This way, each of these readings represent a linear combination of a random set of the original values (i.e. the pixels of the image). Using a mathematical optimization, the complete image can be eventually reconstructed using a number of readings lower than the number of original values (therefore allowing compression), although the process itself is considered “lossy” since a certain amount of information gets lost during the acquisition (nominally, the highest frequencies of the original signal after the application of a transform function). A panchromatic visible image is measured via a Digital Micromirror Device (DMD) on the focal plane which performs a random sampling of the image and by single pixel silicon detector which reads the integrated light flux from the DMD. In other words, the compressive sampling technique delegates the acquisition of spatial coordinates of the image to DMD. By increasing the complexity of the detector, it is possible to add multi or hyper spectral depth to the image without dichroic image splitting or large

*giorgio.pariani@brera.inaf.it

Space Telescopes and Instrumentation 2018: Optical, Infrared, and Millimeter Wave, edited by Makenzie Lystrup, Howard A. MacEwen, Giovanni G. Fazio, Proc. of SPIE Vol. 10698, 106985O
 · doi: 10.1117/12.2312008

spectrometers. Coupling the DMD to a simple spectrometer equipped with a linear detector would allow real time hyperspectral imaging at the pixel level. In this particular implementation, the x,y coordinates are measured by the DMD while the energy spectrum by the spectrometer. By using a multi-band selectable TIR detector[6] it is possible to implement split window algorithms for the retrieval of the exact surface temperature[7]. Complementarily, the implementation of vis-TIR multispectral detectors[8] would allow fusion imaging techniques, merging thermal and visible information at the pixel level. In our actual implementation, the DMD image sampling is performed on the telescope focal plane and the light is then collected and focalized to a single pixel-multispectral detector in the TIR or to a light delivery system, as a light pipe or fiber bundle, to be afterwards processed in a low resolution spectrograph in the vis-NIR.

We will describe in the paper the possibilities offered by this technique, along with all the constraints given by the use of the DMD in the focal plane. The design of the payload, composed by the telescope, the relay system, and the detector/spectrometer in different application cases will be provided.

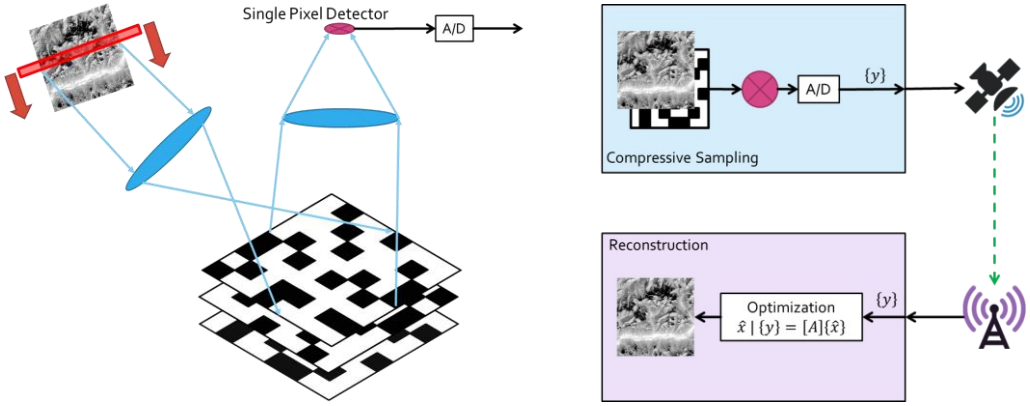

Figure 1: Compressive sensing approach (left); the technique applied to space observations (right).

2. PAYLOAD ARCHITECTURE

In order to exploit the compressive sampling technique, a Digital Micromirror Device (DMD) is considered as spatial light modulator, placed in the telescope focal plane. The DMD samples the focal plane at high speed, and reflects the light in two different channels. In the simplest configuration, all the reflected light is focalized to a single pixel detector, and the image is retrieved with compressive sampling algorithms from the analysis of the intensity fluctuations over time[9]. In more complex configurations, the image or pupil can be reformatted to be further analysed in a low-resolution spectrometer. As shown in Figure 2, the payload is composed by:

- the telescope, collecting the light from space or earth;
- the DMD, placed in the telescope focal plane to create the dynamic masks;
- the post-DMD optics, or relay optics, to focalize the reflected light to the single-pixel detector (channel 1) or to resize the pupil for further light analysis (channel 2);
- the spectrometer or other light analysis instruments.

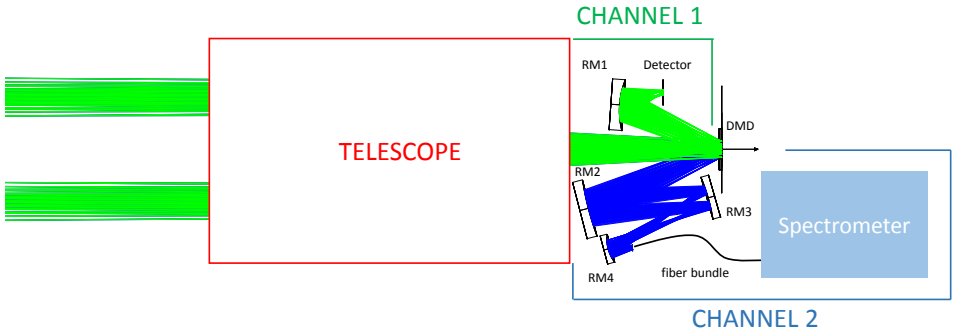

Figure 2: schematics of the payload, where both DMD channels are considered.

2.1 DMD

The DMD is a bistable spatial light modulator, consisting of an array of movable micromirrors mounted over a CMOS memory cell. Each mirror is independently controlled in a binary fashion to steer the reflected light in two opposite channels, where the mechanical tilt angle of any micromirror is usually +/-12 degrees. One or both channels (with the same detector or with detector sensitive in different regions) may be considered when designing the instrument, where half or all light is collected in the two cases, respectively.
Different DMD models are available on the market, with different array size (up to 2560 by 1600 pixels), micromirror dimensions (from 5.4 to 13.6 um) and switching speed, working either in the visible and IR (up to 2.5 um, as function of the cover glass). In order to maximize the swath of the telescope, we considered one of the largest DMD available from Texas Instrument, model DLP9500, with a very high switching speed.
The DMD characteristics are listed hereafter:

Characteristic	**Value**
Array size	1920 x 1080
DMD active area size	20.7 x 11.7
Micromirror pitch	10.8 um
Micromirror tilt angle (relative to flat state)	±12°
Switching time with global reset	56 us (17.8 kHz)

2.2 Telescope

The DMD is governing the paraxial design of the telescope, influencing all the following parameters:

- **field of view (or swath)**: the DMD size is determining the maximum field of view, according to the paraxial equation

$$\vartheta = \frac{x}{f}$$

  where ϑ is the FoV, *x* the DMD size and *f* the telescope focal length.
- **resolution**: the geometrical resolution of the telescope at earth (EGR) is limited by the DMD pixel size *p*, according to

$$EGR = \frac{p\,h}{f}$$

  where *h* the satellite height; the diffraction resolution of the telescope is given by the telescope aperture at the flying altitude

$$EDR = \frac{\lambda\,h}{D}$$

  where λ is the working wavelength and *D* the telescope aperture; by equating the two resolutions, we obtain

$$\frac{f}{D} = F_{\#} = \frac{p}{\lambda} \approx 20\ (VIS)\ or\ 1\ (TIR)$$

  accordingly, the resolution is always limited by diffraction in the TIR (around 10 um), while in the visible is limited by the DMD pixel size.
- **compressive sampling capability**: the larger is the switching speed, the more the intensity data collected in the same time interval and the better is the image reconstruction.
- **working region**: the DMD working region is limited by the micromirror coating reflectivity and by the transmittance of the cover glass. Custom coatings or different cover glasses have to be installed to extend the wavelength range from the UV up to the TIR.

In general, high swath (shorter focal length) is desired to image the earth with fewer overflights. Diffraction and geometrical resolutions are in contrast, but, when moving to thermal IR, diffraction is usually the limiting parameter, and a low F/# (shorter focal length) is preferred. On the contrary, as described hereafter, the DMD is limiting the minimum telescope F/# (longer focal length) due to the necessity to extract the light after reflection. Accordingly, a compromise is required to design a good system in terms of swath, resolution, and efficiency.
To sum up, the DMD size limits the FoV, the DMD micromirror size limits the resolution in the VIS, and the micromirror tilt angle limits the telescope F/#. The telescope parameters of two different application cases are reported hereafter.

Parameter	Case 1	Case 2
satellite height (km)	550000	-
wavelength (um)	0.4 – 0.8; 8.0-12.0	0.36-1.7
f (mm)	400	1325
D (mm)	200	250
DMD size (mm)	20.74x11.67	20.74x11.67
DMD micromirror size (um)	10.8x10.8	10.8x10.8
F/#	2	5.3
FoV (deg)	3.0x1.7	0.9x0.5
earth resolution (m)	40 (VIS), 80 (TIR)	
swath (m)	28.5x16.0	
channels	1 - single pixel	2 - UV, single pixel; - VIS/IR, spectrometer
estimated efficiency	0.1 (detector excluded)	0.78 (UV, detector excluded) 0.16 (VIS/IR, detector excluded)

2.3 Optical design examples

Compressive sampling is enabling imaging in a very wide spectral region with a simple instrument concept. In fact, even if multiple detectors (simple or multispectral) are considered, images are automatically spatially registered, since are all produced by the same mask sequence. The drawback of this approach is that a well defined image must be produced at the DMD plane for the whole band. The very wide spectral band, the large etendue, and, in the first case, the short focal length are determining the complexity of the optical design.

The lack of transparent materials, especially in the first case (0.4 to 12 um), is quite a big problem. Between the few available, we selected Zinc Sulfide, commercially available as Cleartran, as the main material for the large refractive optics. Due to its very high refractive index (larger than 2), reflection losses are important, and an antireflection coating is under study.

In the first case we designed two different telescopes, one based on a two-mirror configuration (both strongly aspherical, with a four lens corrector) and one based on refractive elements (derived from the Riccardi-Honders design, where the primary mirror as an annular Mangin mirror). Given the short F/#, the light is sent to the DMD, placed vertically, with a beam splitter. In this case, only one channel is considered. Optical layouts are reported in Figure 3. The telescopes performances are comparable in the two cases: the RMS spot size is approximately two micromirrors in the visible range, limited by geometrical telescope aberrations, giving a corresponding earth resolution of 40 m, almost uniform throughout the FoV. In the TIR the telescopes become diffraction limited, given by the large increase in wavelenght, and the RMS spot reaches four to five micromirrors, matching the telescope EDR of 80 m.

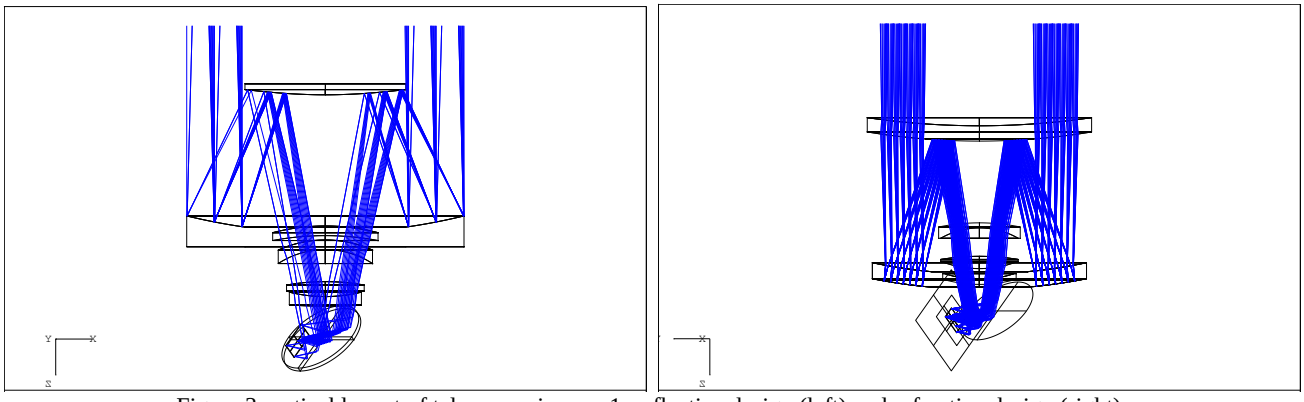

Figure 3: optical layout of telescopes in case 1; reflective design (left) and refractive design (right).

In the second case, given the limited spectral range (0.36-1.7 um), we selected a refractive design based onto the Riccardi-Honders configuration. In fact, no particular limitations exist on the material selection. This configuration provides a good image quality, obtained with a simple construction (all spherical surfaces), and a large back focal distance, necessary to accommodate the refocusing optics after the DMD reflection. In this second case, both DMD

channels are considered. Figure 4 shows the optical layout of the telescopes for different F/#; the long back focal distance is evident, with the drawback of the large internal obstruction.
The optical quality is uniform over all the FoV, with a geometrical RMS spot size smaller than the micromirror size for all the wavelength range. Above 800 nm the telescope is diffraction limited, with a resolution corresponding to the size of two micromirrors.

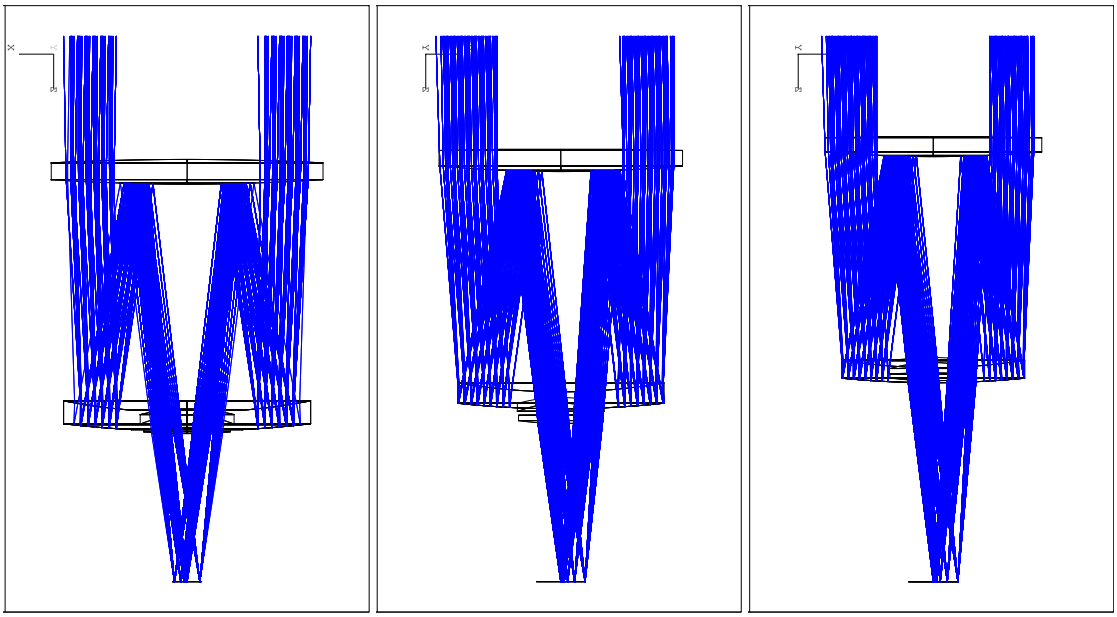

Figure 4: optical layout of telescopes in case two. F/3 (left); F/3.5 (center); F/4 (right).

3. POST-DMD OPTICS

3.1 Light extraction from the DMD

To separate the incoming beam from the reflected beam, a F/# larger than 2.35 (derived from the 24° of optical tilt of the single micromirrors) is required. Considering also the DMD size (the full image field), the limiting F/# is larger than 3. We verified that F/4 is the technological limiting factor to design a telescope with enough back focal distance and a feasible relay system to obtain an efficient light extraction form the DMD.
When smaller F/numbers are required for the telescope operation, light extraction becomes more complicated, and extraction efficiency is always less than unitary. In fact, light is lost after the reflection due to the superposition of the incoming and outcoming beams or to the splitting method.

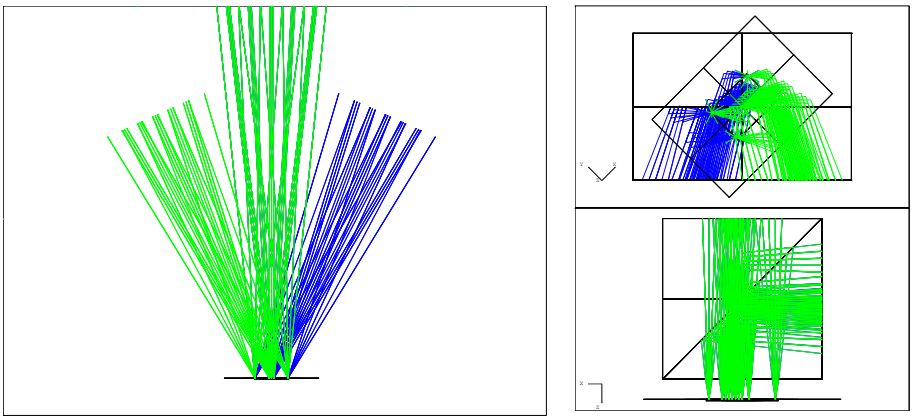

Figure 5: direct beam extraction from the DMD (left); extraction through the right angle beam splitter, top and lateral view (right).

In general, the possible extraction methods are the followings:

- direct extraction after reflection: the ideal solution for efficient two channels operation;
- total internal reflection prism: this is a very efficient solution, possible only when using the single channel and the F/number is larger than 3;
- right angle beam-splitter: this is a possible solution at any F/number, but the overall efficiency is always less than 25% (50% in double reflection).

3.2 Channel 1: single-pixel detector

In the simplest configuration, all the reflected light is focalized to a single pixel detector, with no particular constraints on the optical quality except the overall detector dimensions. In the following example, a single spherical mirror (70 mm diameter, 115 mm RoC) reformats the field to the detector size.

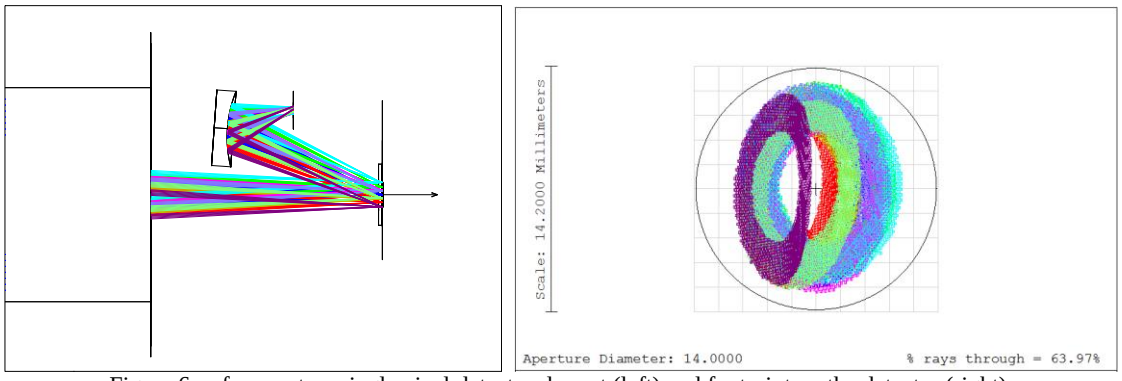

Figure 6: refocuser to a single pixel detector; layout (left) and footprint on the detector (right).

3.3 Channel 2: refocuser and spectrometer

In a more complex configuration, the whole field can be refocused so that the light is injected into a fiber bundle or light pipe, reformatted and processed by a spectrometer. Reformatting is necessary given the large etendue to provide a minimum spectrograph resolution. Actually, an image reduction gives, by the etendue conservation, a decrease in the beam F/#, and a technical limit is easily reached for a fast telescope, accordingly.

We show here the example of a fiber bundle: in order to homogenize any possible light loss, the telescope pupil is reformatted instead of the field to the fiber bundle size and NA. A three mirror achromatic design has been developed, working from 0.42 to 1.7 um. Two mirrors are spherical, the third one is toroidal to easily correct the off-axis aberrations and to enter almost telecentric in the fiber bundle. The first mirror is necessary to fold back the light reflected from the DMD, while the characteristics of the second one are determined by the pupil reduction ratio and position. Figure 7 shows the paraxial design, and Figure 8 the implementation and the simulated pupil image at the fiber bundle entrance.

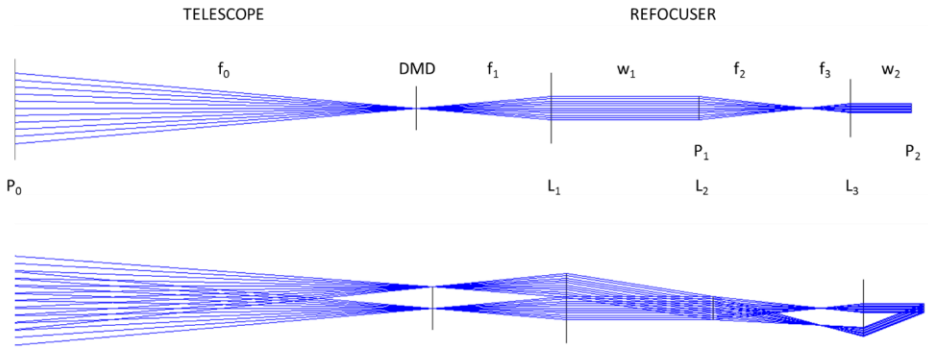

Figure 7: paraxial design of the beam refocuser.

The efficiency of the refocusing system is close to unity, only the reflection losses of the mirrors being present. The coupling efficiency into the fiber bundle and the transmission efficiency of the bundle itself are the main limiting factors. Preliminary calculations of the coupling efficiency show a 20% power loss, while estimations on the bundle transmission efficiency a loss of about 30 to 40%, mainly due to the fill factors of the fibers. Other solutions like the light pipe are now under evaluation. The bundle is reformatted into a rectangular aperture (35x1.5 mm) to be the entrance slit of the spectrometer.

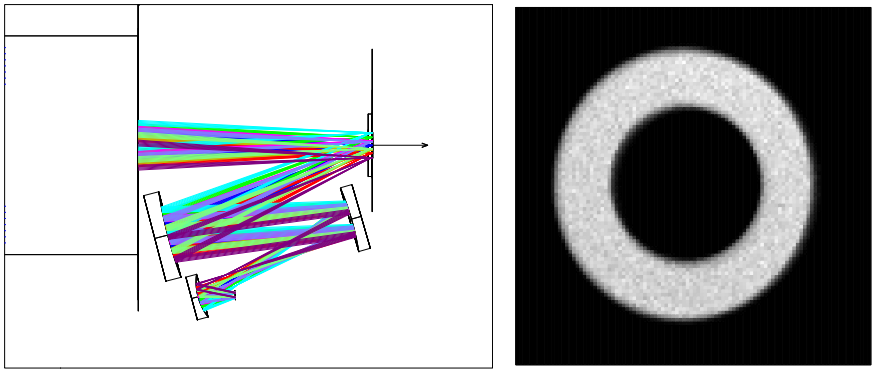

Figure 8: optical layout of the beam refocuser (left) and image of the telescope pupil at the fiber bundle entrance (right).

In the present design the spectrograph covers the visible range from 0.42 to 0.84 um, and the IR up to 1.7 um thanks to an innovative Volume Phase Holographic Grating (VPHG) working on both the first and second orders (developed at the Observatory of Brera in Merate), and a multispectral detector sensitive in two bands, visible and IR (developed at the University of Milano-Bicocca), to match the grating cutoff. The detector is a linear array, with pixels corresponding to the entrance slit size. Accordingly, the compressive sampling algorithm will be applied at each wavelength, to retrieve an hyperspectral image from the blue to the IR.

The spectrograph has been designed adapting the Ebert-Fastie configuration to a transmission diffraction grating, keeping the overall volume as small as possible (Figure 9). Reflective collimator and camera with simple spherical mirrors have been considered, being achromatic on the large spectral range, and are dimensioned to accept the fiber bundle NA. The slit is imaged 1:1 onto the detector; coma is corrected by the symmetric configuration, while the astigmatism is tolerated by the elongated pixel geometry (see the footprints in Figure 10).

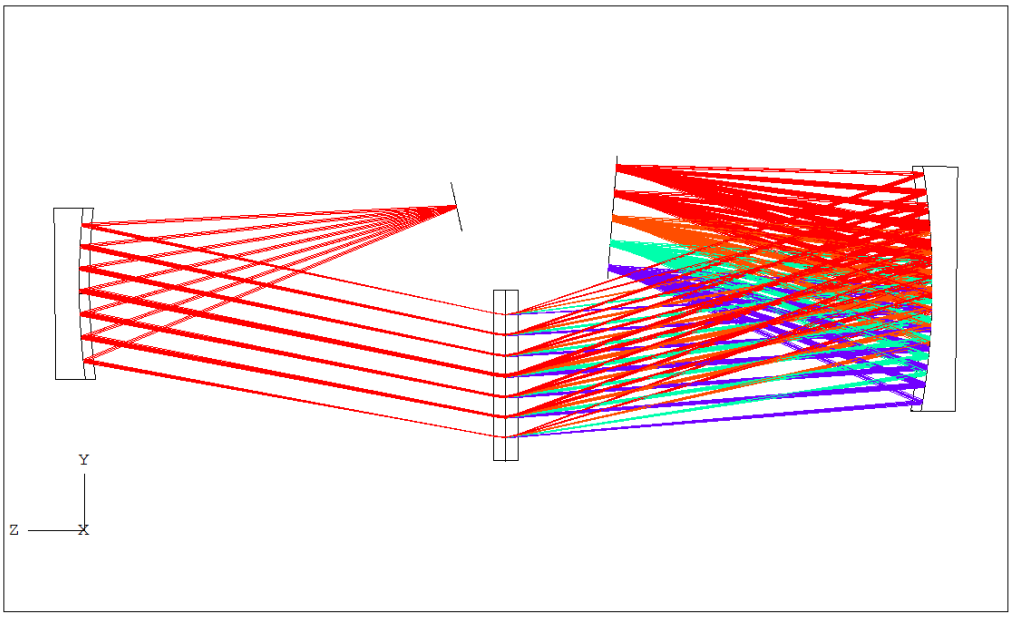

Figure 9: layout of the spectrograph, top view; the fiber bundle is positioned at the entrance slit.

The spectrograph resolving power, calculated with

$$R = \frac{m\, G\, \lambda\, F_{\#\, Coll}\, W}{k\, L}$$

where m is the diffraction order, G the groove density, $F_{\#Coll}$ the collimator F/number, W the grating width, L the slit width, and k a factor to account for the image degradation of the slit width on the detector (about 2.5), is about 20 at 600 nm, and the dispersion is about 10 nm/pixel and 30 nm for resolution element.
The grating has been designed with 330 lines/mm. Thanks to the multispectral detector, selectively sensitive in the visible and IR, the first and second diffraction orders are not separated. The light from 840 nm to 1680 nm, diffracted on the first order, are superimposed to the light from 420 to 840 nm, diffracted on the second order. The detector is then able to recognize the visible and IR intensity on each pixel independently. The spectral formats are reported in Figure 10. The slit image (the resolution element) is linear on the detector (44x44 mm wide, constituted by 44 pixels of 1x44 mm in size) and is about three pixels wide. The grating has been optimized on both orders, reaching a mean diffraction efficiency in the visible of 35% and 70% in the IR (Figure 11).

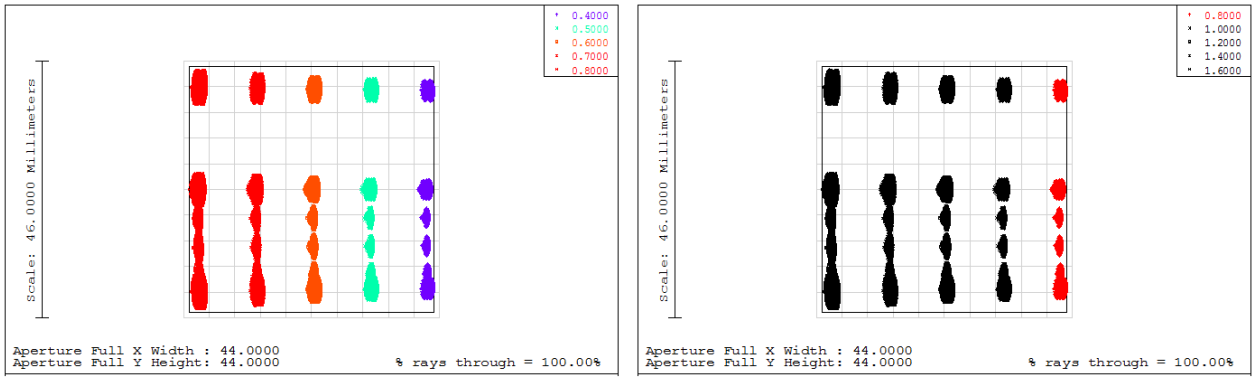

Figure 10: spectral format in the visible (left) and IR (right). The two spectra are superimposed on the detectror.

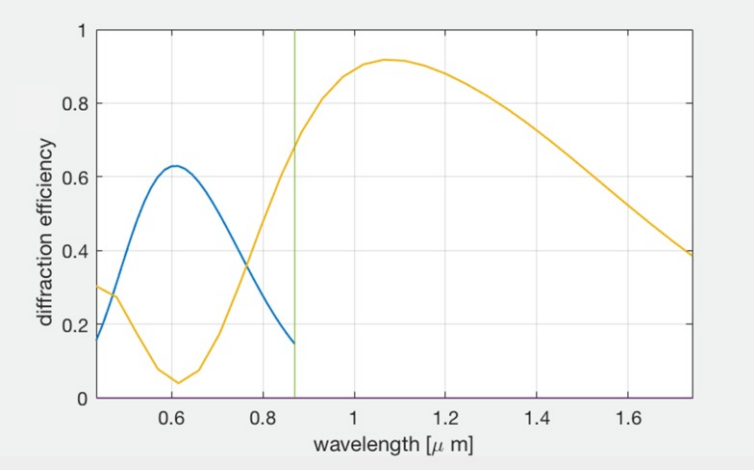

Figure 11: Simulated diffraction efficiencies for the designed VPHG. First (yellow) and second (blue) diffraction orders are displayed. Reflection losses and material absorptions are not taken into account.

3.4 Estimated efficiency

The average efficiency of the two channels is reported hereafter. If a multispectral detector is used in channel 1, multispectral imaging can be performed with high efficiency and a simple architecture. On the contrary, channel 2 suffers from the fiber bundle and the spectrometer efficiencies, given the very large spectral coverage and the

superposition of the two orders. Improvements are possible, but in any case the efficiency is competitive with the state of the art instrumentation.

	Channel 1		Channel 2	
DMD	optics (reflectance and coating)	0.85	optics (reflectance and coating)	0.85
Refocuser	obstruction	1.00	obstruction	1.00
	optics (reflectance)	0.92	optics (reflectance)	0.91
Fiber bundle			acceptance NA	0.82
			collecting area fraction	0.60
Spectrograph			optics (reflectance and coating)	0.94
			grating efficiency	0.45
	detector	TBD	detector	TBD
	TOTAL	**0.78**		**0.16**

4. CONCLUSIONS

We proposed the compressive sampling approach supported by innovative multispectral detectors to obtain hyper- and multi-spectral images in the vis-NIR-TIR bands (0.4-1.7um, and up to 12 um). Possibilities and the constraints given by the use of the DMD in the focal plane have been described, and design examples of the telescope, relay system and spectrometer in two different application cases were provided.

FUNDINGS

This study was supported by CHRISTMAS (Cryosphere High spatial Resolution Images and Snow/ice properties via apparent Thermal inertia obtained from Multispectral Advanced optical Systems campaign) project, ASI N. 2016-11-U.0, and COSMITO (COmpressive Sampling Multispectral Imaging camera for remoTe Observation) project (Regione Lombardia, POR 2014-2020, N.134400).

REFERENCES

[1] "Landsat webpage.", <https://landsat.gsfc.nasa.gov/>.
[2] "Aqua webpage.", <https://aqua.nasa.gov/>.
[3] "Cryosat webpage.", <https://www.esa.int/Our_Activities/Observing_the_Earth/CryoSat>.
[4] "Sentinel webpage.", <https://sentinel.esa.int/web/sentinel/home>.
[5] Candès, E., Romberg, J., "Sparsity and incoherence in compressive sampling," Inverse Probl. **23**(3), 969–985 (2007).
[6] Lu, X., Vaillancourt, J., Meisner, M. J., "An electrically-controllable multi-spectral quantum dot infrared photodetector with high photodetectivity," Proc. SPIE(6542) (2007).
[7] Sobrino, J. A., Jiménez-Muñoz, J. C., "Minimum configuration of thermal infrared bands for land surface temperature and emissivity estimation in the context of potential future missions," Remote Sens. Environ. **148**, 158–167, Elsevier (2014).
[8] Frigerio, J., Isella, G., Bietti, S., Sanguinetti, S., "Multispectral imaging sensors integrated on silicon," SPIE Newsroom, 2–4 (2013).
[9] Romberg, J., "Imaging via Compressive Sampling," IEEE Signal Process. Mag. **25**(2), 14–20 (2008).